Progress In Electromagnetics Research C, Vol. 28, 195–207, 2012

DESIGN OF CPW-FED DUAL-BAND CIRCULARLY-POLARIZED ANNULAR SLOT ANTENNA WITH TWO PERTURBATION STRIPS

Q. Chen*, H.-L. Zheng, J.-H. Hu, and S.-G. Jiang

National Laboratory of Antennas and Microwave Technology, Xidian University, Xi'an, Shaanxi 710071, P. R. China

Abstract—A new CPW-fed dual-band circularly-polarized(CP) annular slot antenna with two perturbation strips is proposed. The structure of the annular slot, along with two concentric annular-ring patches, can achieve dual-band input impedance matching. And circular polarization at the operation bands can be achieved by using the two perturbation strips placed on the backside of the antenna. To reduce the resonant frequencies, a third strip protruded from the ground plane is introduced. Both the simulated and measured results show that the impedance bandwidths determined by 10-dB return loss are about 29.1% for the lower band (1.92–2.61 GHz) and 12.1% for the upper band (3.21–3.65 GHz). And the AR bandwidths are about 7.5% and 11.0%, respectively.

1. INTRODUCTION

Due to the demands of wireless communication services, dual-band antennas are widely used. The dual-band antennas can work at the specific frequency band, such as 3G wideband code division multiple access (WCDMA) mobile service from 1.92 to 2.17 GHz, world interoperability for microwave access (WiMAX) service from 3.4 to 3.69 GHz, the wireless local area network (WLAN) for IEEE 802.11a in the USA (5.15 to 5.35 GHz, 5.725 to 5.825 GHz), and HIPERLAN/2 in Europe (5.15 to 5.35 GHz, 5.47 to 5.725 GHz). During the last decade, many types of antennas have been developed to deal with dual designs, among which the printed CPW-fed slot antenna is confirmed a promising candidate due to its advantages of

Received 16 February 2012, Accepted 6 April 2012, Scheduled 11 April 2012
* Corresponding author: Qiong Chen (chenqiong2100@163.com).

wide bandwidths, light weight, low profile, and easy integration with monolithic microwave integrated circuits(MMICs) [1]. Generally, one or two circular or rectangular-ring slots can be etched in the ground plane to generate dual or multi-band performance [1–4]. In [5], a CPW-fed equilateral triangular-ring slot antenna is proposed to attain dual band performance. All of these antennas mentioned in [1–5], however, are linearly polarized (LP) for they are symmetrically excited. To achieve CP operation, another orthogonal LP wave of equal amplitude and 90° phase difference (PD) should be excited. And the orthogonal LP wave can be realized by using special asymmetrical exciting designs [6–10] or introducing weak perturbation structures [11–14]. Commonly, deformed-bent [6, 7], L-shaped [8, 9] or V-shaped [10] coupling feedlines are popular structures used as asymmetrical exciting designs to realize CP operation. As an alternative technology to create CP waves, an L-shaped strip is etched on the backside of a coplanar waveguide as a perturbation stub in [14]. By using this technique, 8.3% of AR bandwidth can be achieved. In [15, 16], asymmetrical exciting designs and weak perturbation structures are combined to acquire CP performance.

Typically, the basic steps to design a dual frequency CP antenna are firstly getting dual band operation and then realizing 3-dB ARs at the working bands. During the procedure, one of the most difficult challenges is to make sure that the impedance bands enclose the CP bands, which requires the antennas frequency adjustable. In [1, 2], a strip protruded from the ground is introduced to decrease the resonant frequencies without changing other dimensions of the antennas. As an alternative method, etching gaps or grooves on the radiating patches are introduced in [17, 18] to tune each resonant frequency independently.

In this article, a new CPW-fed dual frequency CP circular slot antenna is proposed. The outer annular-ring patch is used to excite the annular slot, and several resonant modes can be achieved. To decrease the two resonant frequencies, a protruded strip from the ground plane is applied to this structure. The dual-band CP characteristic can be obtained by placing two strips on the backside of the antenna. Furthermore, a gap etched in the ground plane is used to guarantee the CP bands completely enclosed by the impedance bands. As a result, the 3-dB ARs cover 1.95–2.12 GHz and 3.25–3.62 GHz. Thus, the proposed antenna can be suitable for WCDMA (2-GHz) and Wimax (3.5-GHz) application application. Details of the antenna design and the measured results of the constructed prototype are presented and discussed.

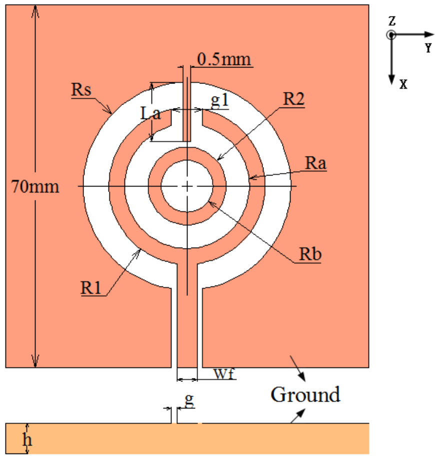

Figure 1. The basic structure of the proposed antenna.

2. ANTENNA DESIGN AND DISCUSSION

2.1. The Basic Structure for Dual Band Operation

The geometry of the proposed antenna for dual-band or multiple-band operation is illustrated in Figure 1. The antenna is printed on the 1.6-mm FR4 substrate of a relative permittivity 4.4 and a loss tangent 0.02. The ground plane is chosen to be square with a size of $70\,\mathrm{mm} \times 70\,\mathrm{mm}$. A circular slot etched in the centre of the ground plane has a radius of R_s. Two concentric annular-ring patches, of which the outer radii are R_1 and R_2, respectively, are embedded in the slot. And the inner radii of the annular-ring patches are R_a and R_b, respectively. A gap with a length of g_1 is loaded in the outer annular-ring patch. To reduce the resonant frequencies, a protruded strip from the ground plane into the slot is used. The strip has a length of L_a and a width of 0.5 mm. In addition, the antenna is fed by a 50-Ω CPW composed of a signal strip of width $W_f = 4\,\mathrm{mm}$ and two identical gaps of width $g = 0.35\,\mathrm{mm}$.

For the conventional circular slot antenna, the lower resonant frequency mainly depends on the radius R_s of the circular slot and the outer radius R_1 of the outer annular-ring patch. And the higher resonant frequency can be adjusted by modifying the value of R_2. In this proposed antenna, the introduction of the strip protruded from the ground plane can greatly reduce the resonant frequencies [1].

Figure 2 shows the return losses varying with the length L_a of the protruded strip. It can be seen that the annular slot antenna without the protruded strip can generate three modes, corresponding to the

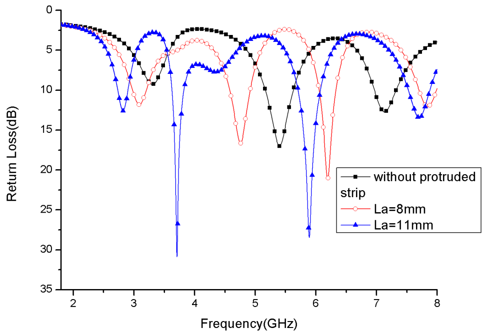

Figure 2. Simulated return losses varying with L_a. (Geometry parameters: $R_s = 20$ mm, $R_1 = 15$ mm, $R_2 = 7.5$ mm, $R_a = 12$ mm, $R_b = 5$ mm, $g_1 = 6$ mm.).

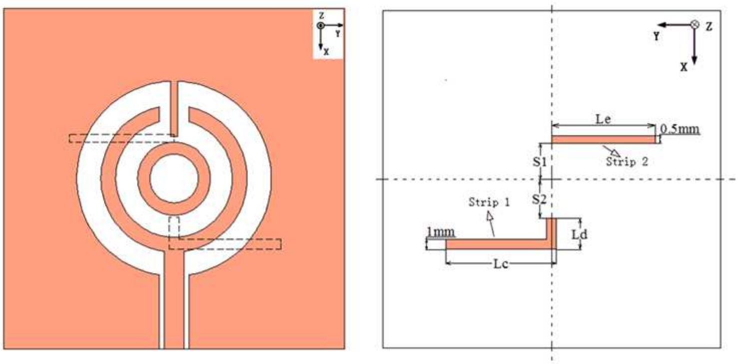

(a) Top view. (b) Bottom view.

Figure 3. The structures and locations of the two strips on the backside.

frequencies of 3.3 GHz, 5.5 GHz, and 7.1 GHz, respectively. Introducing the protruded strip can reduce all the three resonant frequencies and enhance the impedance matching at the same time. And this effect becomes clearer when the length L_a of the protruded strip increases.

2.2. The Design for CP Operation

Since the antenna mentioned above is symmetrically excited, only LP radiation can be created. To achieve CP operation, extra perturbation structures should be added. In this proposed antenna, two strip lines on the backside are used to provide an orthogonal LP wave.

Figure 3 shows the structure of the two strips (denoted by Strip 1 and 2) for CP operation. They are placed on the backside of the antenna. Strip 1 with inverted-L shape has lengths of L_d in the x direction and L_c in the y direction. And its width is 1 mm. The length of Strip 2 is L_e, and its width is chosen to be 0.5 mm. The locations of the two strips are also shown in Figure 3(b). During the process of design, we have found that the locations of the two strips should be carefully chosen.

As the first step to achieve CP operation, we put an x-directed strip line on the left bottom backside, as shown in Figure 4 (denoted by Type 1 antenna). It can be seen that with the introduction of the strip line, minimum ARs can be achieved at 2.24 GHz and 3.18 GHz, respectively. To enhance the CP operation at higher band, an additional x-directed strip line with a length L_d is added to the former strip line, making up an inverted L-shaped line (denoted by Type 2 antenna). From Figure 4, we can see that minimum ARs of Type 2 antenna at higher band can be achieved at 3.25 GHz and 3.55 GHz, respectively. Once designed properly, 3-dB AR bandwidth at

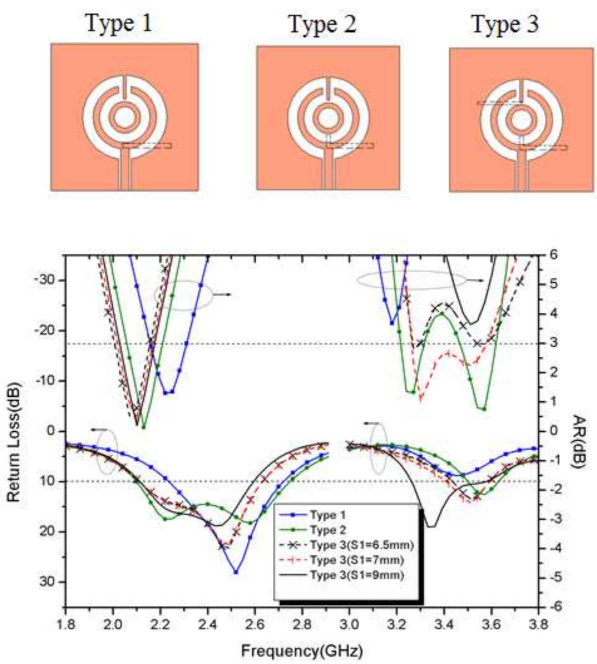

Figure 4. The comparison of the return losses and the boresight ARs for the three types of antennas. (Geometry parameters: $R_s = 20$ mm, $R_1 = 15$ mm, $R_2 = 7.5$ mm, $R_a = 12$ mm, $R_b = 5$ mm, $g_1 = 6$ mm, $L_a = 11.4$ mm, $L_c = 22.5$ mm, $L_d = 6$ mm, $L_e = 21$ mm, $S_2 = 8$ mm.).

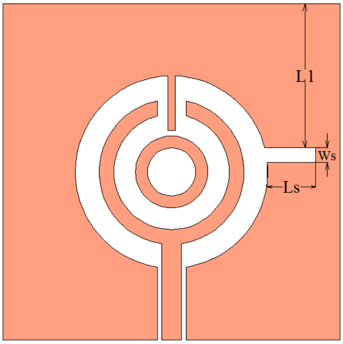

Figure 5. Antenna with ground plane loaded groove.

higher band can be broadened. Thus, we put another y-directed strip line on the upper left corner backside (denoted by Type 3 antenna). It is clear that the 3-dB AR bandwidth of Type 3 antenna at higher band can be adjusted by changing the distance S_1 between Strip 2 (denoted in Figure 3) and y axial.

It is worth noting that the lower operating band does not completely cover the AR band. The method to solve this problem will be discussed in the next section.

2.3. Final Structure of Proposed Antenna with Groove Loaded in Ground Plane

To make sure that the lower operating band encloses the AR band, we should find the way to adjust the first frequency band without affecting the other working band and CP operation. For this annular-ring structure, cutting grooves or gaps in appropriate locations of ground plane or patches are a useful way to tune one resonant frequency independently [17]. Figure 5 shows the dimension and location of the groove loaded in the ground plane. The length of the groove is L_s, and width is W_s. The distance between the upper edge of the groove and the ground plane is L_1.

Figure 6 shows the effects of the groove on return loss and ARs of the antenna. It is observed that the lower operating band decreases apparently when the length L_s of the groove increases. And the higher operating band at 3.2–3.6 GHz remains relatively stable. It also shows that the ARs at 3.2–3.6 GHz change little, while at lower band, the frequencies corresponding to the 3-dB ARs decrease slightly. And when $Ls = 10\,\mathrm{mm}$, both the impedance bands enclose the ARs bands.

It should be mentioned that though 10-dB return loss is obtained

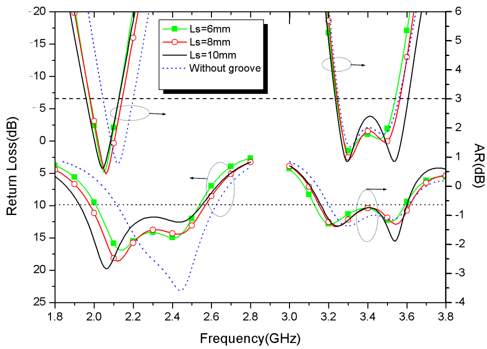

Figure 6. The effect of the groove on return losses and boresight ARs. (Geometry parameters: $Rs = 20\,\mathrm{mm}$, $R_1 = 15\,\mathrm{mm}$, $R_2 = 7.5\,\mathrm{mm}$, $R_a = 12\,\mathrm{mm}$, $R_b = 5\,\mathrm{mm}$, $g_1 = 6\,\mathrm{mm}$, $L_a = 11.4\,\mathrm{mm}$, $L_c = 22.5\,\mathrm{mm}$, $L_d = 6\,\mathrm{mm}$, $L_e = 21.5\,\mathrm{mm}$, $S_1 = S_2 = 8\,\mathrm{mm}$, $L_s = 10\,\mathrm{mm}$, $L_1 = 30\,\mathrm{mm}$, $W_s = 2\,\mathrm{mm}$.).

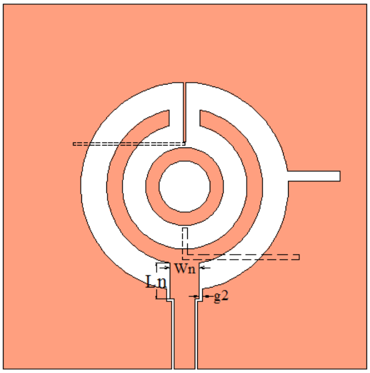

Figure 7. Final structure of the proposed antenna along with the tuning stub.

at the band of 3.2–3.6 GHz and that the impedance matching performance is not quite satisfactory. To further enhance impedance matching, a tuning stub is embedded between the annular-ring patch and feeding strip. Figure 7 shows the final structure of the proposed antenna along with the tuning stub. The length of the stub is L_n, and the width is W_n. And the width of the gaps between the stub and ground plane is g_2. The photograph of the proposed antenna is given in Figure 8.

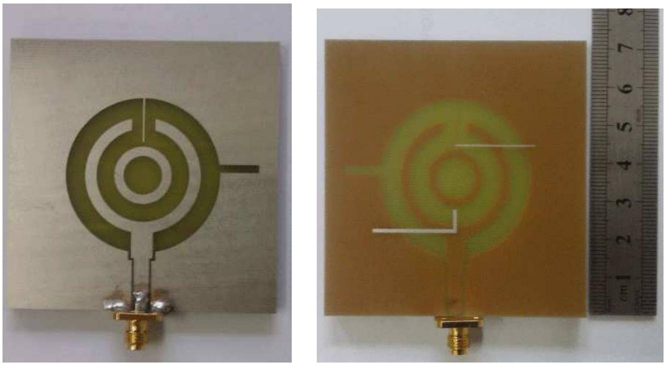

(a) Main view (b) Bottom view

Figure 8. The photograph of the fabricated antenna prototype.

Table 1. Dimensional parameters of proposed antenna.

Parameter	R_s	R_1	R_2	R_a	R_b	g_1	L_a	L_s	L_c
Value (mm)	20	15	7.5	12	5	6	11.4	10	22.5
Parameter	L_d	L_e	L_1	W_s	S_1	S_2	L_n	W_n	g_2
Value (mm)	6	21.5	30	2	8	8	10	5.6	0.6

3. PARAMETRIC STUDY OF THE PROPOSED DUAL-BAND CP ANTENNA

Since many parameters affect the performance of proposed antenna, here we only focus on studying the effects of the inner circular-ring patch(R_2, R_b) and the strips on the backside on the impedance matching and circular polarization performance. Other parameters that have not been mentioned are fixed at the values shown in Table 1. Meanwhile, the Ansoft HFSS simulation package is used to perform the design and study process.

Figure 9 reveals the return losses and ARs at different values of R_2 and R_b. To simplify the discussion, we keep $R_2 - R_b = 2.5$ mm. The figure illustrates that different R_2 and R_b will result in a variation of return losses at upper frequency band. And the resonant frequency at lower band remains stable. Meanwhile, the CP performance at upper band is sensitive to the values of R_2 and R_b. When R_2 decreases from 7.5 mm to 6 mm or increases from 7.5 mm to 8 mm, the CP performance will dramatically become poor at upper band. And the 10-dB impedance band will become narrower. If we cross out the inner

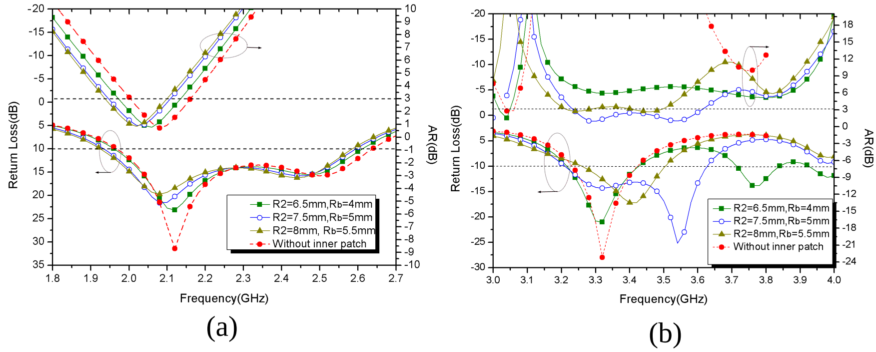

Figure 9. The effects of the inner patch on performance of the proposed antenna: (a) at lower band; (b) at higher band.

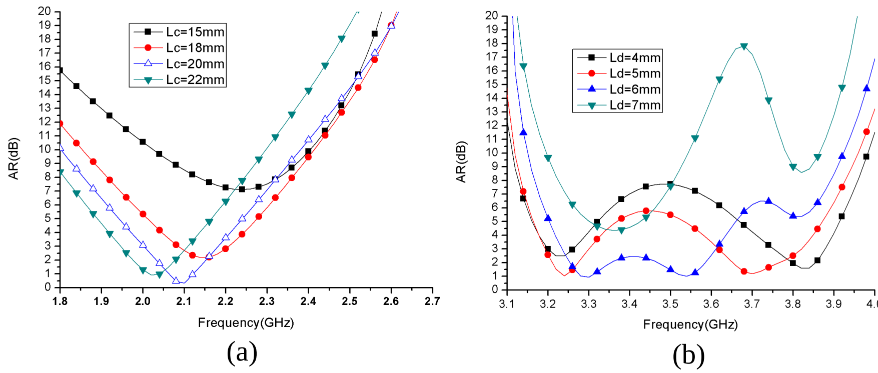

Figure 10. The effects of the L-shaped strips (Strip 1) on CP performance: (a) the ARs at lower band varying with L_c; (b) the ARs at higher band varying with L_d.

ring patch, i.e., $R_2 = R_b = 0\,\text{mm}$, the CP operation at 3.23–3.6 GHz will disappear but can still be achieved at lower band. Thus, it can be concluded that the inner circular-ring patch takes an important role in the generation of the CP wave at the band of 3.23–3.6 GHz.

Figure 10(a) displays the boresight ARs at lower band varying with the length L_c of Strip 1 in the y direction. As shown in Figure 10(a), the AR decreases as L_c increases from 15 mm to 22 mm. And the frequency corresponding to the minimum AR becomes lower. Figure 10(b) shows ARs at upper band varying with the length L_d of Strip 1 in the x direction. It shows that the ARs at upper band are sensitive to L_d. A slight variation of L_d from 6 mm may result in a poor CP performance at this band. When L_d =6 mm, the minimum AR can be found at 3.3 GHz and 3.55 GHz.

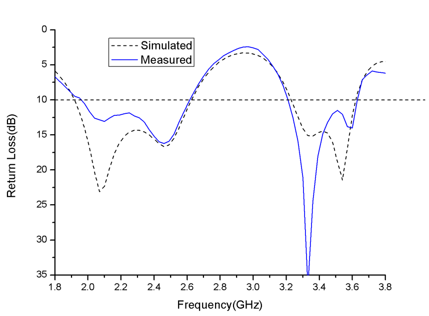

Figure 11. The simulated and measured results of return losses.

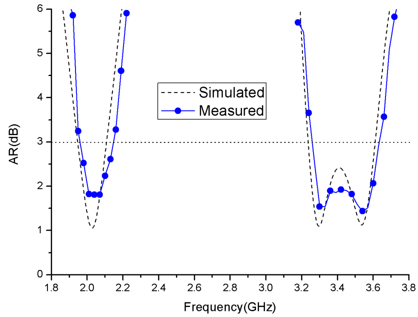

Figure 12. The simulated and measured results of boresight ARs.

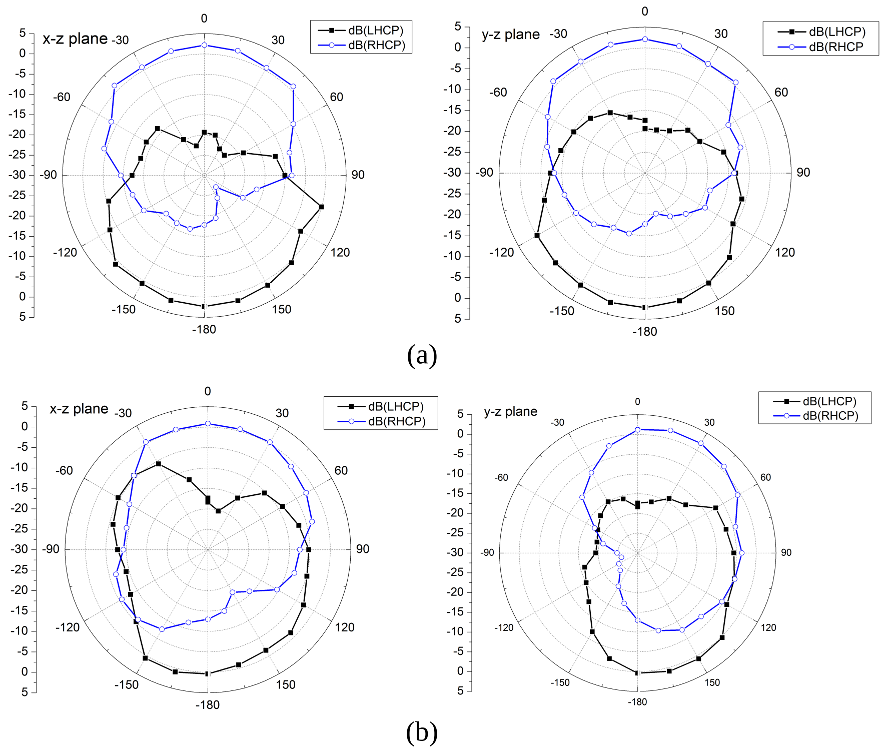

Figure 13. Measured radiation patterns of the antenna at (a) 2 GHz, (b) 3.5 GHz.

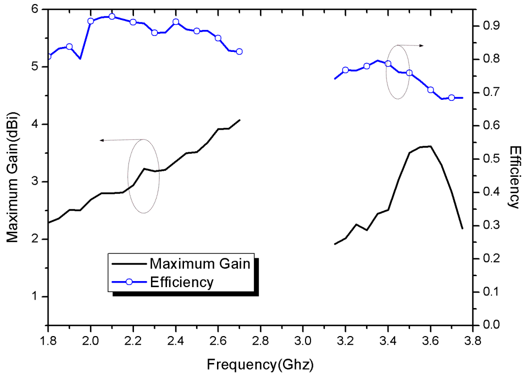

Figure 14. Measured results of radiation efficiency and maximum gains.

4. EXPERIMENT RESULTS AND DISCUSSION

To verify the design of the antenna, an antenna prototype of the proposed antenna shown in Figure 8 is fabricated based on the optimized dimensions listed in Table 1 and measured by Agilent E5071C vector network analyzer.

Figure 11 exhibits the comparison between the simulated and measured return losses and shows that there is a reasonably good agreement between simulated and measured results. Both of them imply that dual frequency bands cover 1.92–2.61 GHz and 3.21–3.65 GHz, respectively.

Figure 12 shows the simulated and measured results of ARs varying with frequency. It can be seen that the 3-dB ARs are attained at the frequency of 1.95–2.11 GHz and 3.23–3.61 GHz, which are enclosed by the 10-dB impedance band.

The measured radiation patterns at 2 GHz and 3.5 GHz are demonstrated in Figure 13. It can be found that the patterns at the two frequencies are RHCP for $z > 0$ and LHCP for $z < 0$. It also can be seen that the wide 3-dB beamwidth can be attained at 2 GHz, around 90°. At 3.5 GHz, the main beam direction shifts slightly away from the zenith. As a result, the 3-dB beamwidth is about 30°.

Figure 14 displays the measured maximum gains (not including losses arising from impedance mismatch) and radiation efficiency versus frequency. The use of low-loss FR4 substrate can lead to a high efficiency at operation bands, as can be seen in the figure. Figure 14 also shows that the maximum gains are between 2–4 dBi at the working frequency bands.

5. CONCLUSION

A dual-band circularly polarized CPW-fed slot antenna with two concentric annular-ring patches and two perturbation strips is proposed and fabricated. The annular slot along with the two annular-ring patches embedded in the ground plane can support dual input impedance matching bands. The protruded strip from the ground plane can reduce the resonant frequencies. And the two perturbation strips contributes to generation of CP radiation at the dual bands. The groove cutting in the inner edge of ground plane can ensure the impedance bands enclose the AR bands. Both the simulated and measured results show that the 10-dB impedance bands cover 1.92–2.61 GHz at lower band and 3.21–3.65 GHz at higher band. The 3-dB AR of the proposed antenna can be attained at the frequency bands of 1.95–2.11 GHz and 3.23–3.61 GHz respectively. The maximum gains are about 2-4dBi at the working bands. As a result, the antenna can be applied to modern wireless communication application, such as WCDMA(1.92–2.17 GHz) and Wimax (3.4–3.69 GHz).

REFERENCES

1. Chiang, M.-J., T.-F. Hung, J.-Y. Sze, and S.-S. Bor, "Miniaturized dual-band CPW-fed annular slot antenna design with arc-shaped tuning stub," *IEEE Transactions on Antennas and Propag.*, Vol. 58, No. 11, Nov. 2010.
2. Llorens, D., P. Otero, and C. Camacho-Peñalosa, "Dual-band, single CPW port, planar-slot antenna," *IEEE Transactions on Antennas and Propag.*, Vol. 51, No. 1, 137–139, Jan. 2003.
3. Chen, J.-S., "Dual-frequency annular-ring slot antennas fed by CPW feed and microstrip line feed," *IEEE Transactions on Antennas and Propag.*, Vol. 53, No. 1, Jan. 2005.
4. Chen, J.-S., "Triple-frequency annular-ring slot antennas fed by CPW and microstrip Line," *IEEE Antennas and Propag. Society International Symposium*, Vol. 2, 557–560, Jun. 2003.
5. Chen, J.-S., "Studies of CPW-fed equilateral triangular-ring slot antennas and triangular-ring slot coupled patch antennas," *IEEE Transactions on Antennas and Propag.*, Vol. 53, No. 7, Jul. 2005.
6. Sze, J.-Y., C.-I. G. Hsu, M.-H. Ho, Y.-H. Ou, and M.-T. Wu, "Design of circularly polarized annular-ring slot antennas fed by a double-bent microstrip line," *IEEE Transactions on Antennas and Propag.*, Vol. 55, No. 11, Nov. 2007.

7. Sze, J.-Y. and W. -H. Chen, "Axial-ratio bandwidth enhancement of a microstrip-line-fed circularly polarized annular-ring slot antenna," *IEEE Transactions on Antennas and Propag.*, Vol. 59, No. 7, Jul. 2011.
8. Row, J.-S., "The design of a squarer-ring slot antenna for circular polarization," *IEEE Transactions on Antennas and Propag.*, Vol. 53, No. 6, Jun. 2005.
9. Chen, Y.B., X. F. Liu, Y. C. Jiao, and F. S. Zhang, "CPW-fed broadband circularly polarized square slot antenna," *Electron. Lett.*, Vol. 42, No. 19, Sep. 2006.
10. Row, J.-S., T.-Y. Lee, and M.-Y. Chen, "Circularly-polarized ring slot antenna fed by a V-shaped coupling strip," *IEEE Transactions on Antennas and Propag.*, 2011.
11. Wong, K.-L., C.-C. Huang, and W.-S. Chen, "Printed ring slot antenna for circular polarization," *IEEE Transactions on Antennas and Propag.*, Vol. 50, No. 1, Jan. 2002.
12. Sze, J.-Y., K.-L. Wong, and C.-C. Huang, "Coplanar waveguide-fed square slot antenna for broadband circularly polarized radiation," *IEEE Transactions on Antennas and Propag.*, Vol. 51, No. 8, Aug. 2003.
13. Sze, J.-Y. and C.-C. Chang, "Circularly polarized square slot antenna with a pair of inverted-L grounded strips," *IEEE Antennas and Wireless Propag. Lett.*, Vol. 7, 2008.
14. Chang, T.-N., "A CPW-fed annular slot-antenna with an L-shaped strip," *Microwave and Opt. Technol. Lett.*, Vol. 53, No. 12, 2821–2827, Dec. 2011.
15. Sze, J.-Y. and S.-P. Pan, "Design of broadband circularly polarized square slot antenna with a compact size," *Progress In Electromagnetics Research,* Vol. 120, 513–533, 2011.
16. Rezaeieh, S. A. and M. Kartal, "A New triple band circularly polarized square slot antenna design with crooked T and F-shape strips for wireless applications," *Progress In Electromagnetics Research*, Vol. 121, 118, 2011.
17. Jhamb, K., L. Li, and K. Rambabu, "Frequency adjustable microstrip annular ring patch antenna with multi-band characteristics," *IET Microw. Antennas Propag.*, Vol. 5, No. 12, 1471–1478, 2011.
18. Latif, S. I. and L. Shafai, "Polarization characteristics of multiband loaded microstrip annular ring antennas," *IEEE Transactions on Antennas and Propag.*, Vol. 57, No. 9, Sep. 2009.